We are IntechOpen, the world's leading publisher of Open Access books
Built by scientists, for scientists

6,900
Open access books available

185,000
International authors and editors

200M
Downloads

154
Countries delivered to

Our authors are among the

TOP 1%
most cited scientists

12.2%
Contributors from top 500 universities

CLARIVATE ANALYTICS
BOOK CITATION INDEX
INDEXED

WEB OF SCIENCE™

Selection of our books indexed in the Book Citation Index
in Web of Science™ Core Collection (BKCI)

Interested in publishing with us?
Contact book.department@intechopen.com

Numbers displayed above are based on latest data collected.
For more information visit www.intechopen.com

Programmable All-Fiber Optical Pulse Shaping

Antonio Malacarne[1], Saju Thomas[2], Francesco Fresi[1,2], Luca Potì[3],
Antonella Bogoni[3] and Josè Azaña[2]
[1]Scuola Superiore Sant'Anna, Pisa,
[2]Institut National de la Recherche Scientifique (INRS), Montreal, QC,
[3]Consorzio Nazionale Interuniversitario per le Telecomunicazioni (CNIT), Pisa,
[1,3]Italy
[2]Canada

1. Introduction

Techniques for the precise synthesis and control of the temporal shape of optical pulses with durations in the picosecond and sub-picosecond regimes have become increasingly important for a wide range of applications in such diverse fields as ultrahigh-bit-rate optical communications (Parmigiani et al., 2006; Petropoulos et al., 2001; Oxenlowe et al., 2007; Otani et al., 2000), nonlinear optics (Parmigiani et al., 2006 b), coherent control of atomic and molecular processes (Weiner, 1995) and generation of ultra-wideband RF signals (Lin & Weiner, 2007). To give a few examples, (sub-)picosecond flat-top optical pulses are highly desired for nonlinear optical switching (e.g. for improving the timing-jitter tolerance in ultrahigh-speed optical time domain de-multiplexing (Parmigiani et al., 2006; Petropoulos et al., 2001; Oxenlowe et al., 2007)) as well as for a range of wavelength conversion applications (Otani et al., 2000); high-quality picosecond parabolic pulse shapes are also of great interest, e.g. to achieve ultra-flat self-phase modulation (SPM)-induced spectral broadening in super-continuum generation experiments (Parmigiani et al., 2006 b). For all these applications, the shape of the synthesized pulse needs to be accurately controlled for achieving a minimum intensity error over the temporal region of interest. The most commonly used technique for arbitrary optical pulse shaping is based on spectral amplitude and/or phase linear filtering of the original pulse in the spatial domain; this technique is usually referred to as 'Fourier-domain pulse shaping' and has allowed the programmable synthesis of arbitrary waveforms with resolutions better than 100fs (Weiner, 1995). Though extremely powerful and flexible, the inherent experimental complexity of this implementation, which requires the use of very high-quality bulk-optics components (high-quality diffraction gratings, high-resolution spatial light modulators etc.), has motivated research on alternate, simpler solutions for optical pulse shaping. This includes the use of integrated arrayed waveguide gratings (AWGs) (Kurokawa et al., 1997), and fiber gratings (e.g. fiber Bragg gratings (Petropoulos et al., 2001), or long period fiber gratings (Park et al. 2006)). However, AWG-based pulse shapers (Kurokawa et al., 1997) are typically limited to time resolutions above 10ps. The main drawback of the fiber grating approach (Petropoulos et al., 2001; Park et al. 2006) is the lack of programmability: a grating device is designed to realize a single pulse shaping operation over a specific input pulse (of prescribed wavelength and bandwidth) and once

the grating is fabricated, these specifications cannot be later modified. Recently, a simple and practical pulse shaping technique using cascaded two-arm interferometers has been reported (Park & Azaña, 2006). This technique can be implemented using widely accessible bulk-optics components and can be easily reconfigured to synthesize a variety of transform-limited temporal shapes of practical interest (e.g. flat-top and triangular pulses) as well as to operate over a wide range of input bandwidths (in the sub-picosecond and picosecond regimes) and center wavelengths. However, this solution presents all the drawbacks due to a free-space solution where it is needful to strictly set the relative time delay inside each interferometer in order to "program" different obtainable pulse shapes. Therefore the pursuit of an integrated (fiber) pulse shaping solution, including full compatibility with waveguide/fiber devices, which can be able to provide the additional functionality of electronic programmability, manifests to be useful for a lot of different application fields. For this reason a programmable fiber-based phase-only spectral filtering setup has been recently introduced (Azaña et al., 2005; Wang & Wada, 2007). In the next section the working principle of this spectral phase-only linear filtering approach is discussed and an improvement of the solution reported in (Azaña et al., 2005) is presented and widely investigated.

2. Programmable all-fiber optical pulse shaper

A pulse shaper can be easily described in the spectral domain as an amplitude and/or phase filter. Using linear system theory it is possible to consider an input signal $e_{in}(t)$ whose frequency spectrum is $E_{in}(\omega)$ as reported in Fig. 1, and the corresponding output spectrum $E_{out}(\omega)$. The pulse shaper is represented by a filter transfer function $H(\omega)$ so that:

$$E_{out}(\omega) = E_{in}(\omega) \cdot H(\omega) = \Im\{e_{out}(t)\} \tag{1}$$

where $H(\omega)$ is found out so that the output temporal shape $e_{out}(t) = u(t)$, with $u(t)$ the desired target intensity profile.

Previous solutions are based on amplitude-only filtering (Dai & Yao, 2008), amplitude and phase filtering (Petropoulos et al., 2001; Weiner, 1995; Park et al., 2006; Azaña et al., 2003), or phase-only filtering (Azaña et al., 2005; Wang & Wada, 2007; Weiner et al., 1993). In term of power efficiency phase filtering is preferred since the energy is totally preserved with respect to amplitude only or amplitude and phase filtering where some spectral components are attenuated or canceled. Avoiding any amplitude filtering, in principle we may achieve an energy lossless pulse shaping. Moreover, if only the output temporal intensity profile is targeted, keeping its temporal phase profile unrestricted, a phase-only filtering offers a higher design flexibility, even if obviously it rules out the possibility to obtain a Fourier transform-limited output signal or an output phase equal to the input one. Then, with phase-only filtering we are able to carry out an arbitrary temporal output phase but with a programmable *desired* temporal output intensity profile.

In this case the system is represented by a phase-only transfer function $M(\omega) = K\,e^{j\Phi(\omega)}$, where the design task is to look for $\Phi(\omega)$ such that:

$$\Im^{-1}\{M(\omega) \cdot E_{in}(\omega)\} = u(t) \tag{2}$$

The very interesting fiber-based solution for programmable pulse shaping proposed in (Azaña et al., 2005) and used in (Wang & Wada, 2007) is based on time-domain optical

phase-only filtering. This method originates from the most famous technique for programmable optical pulse shaping, based on spatial-frequency mapping (Weiner et al., 1993).
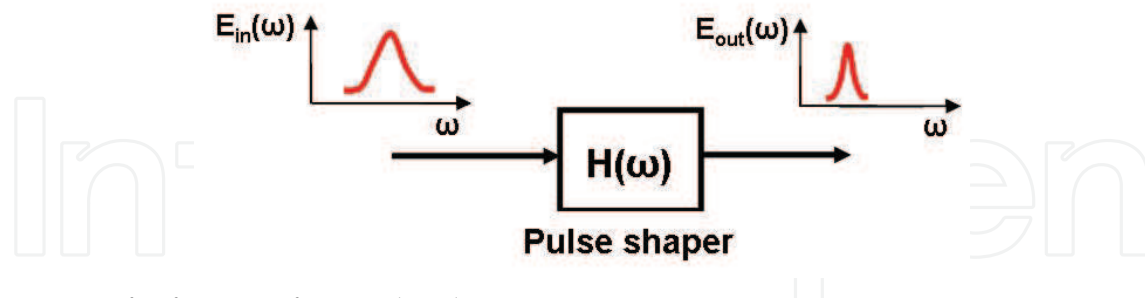

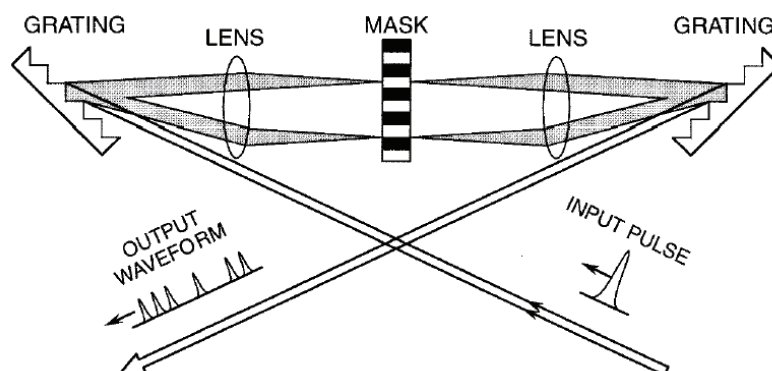Fig. 1. Transfer function for a pulse shaper

Fig. 2. Spatial-domain approach for shaping of optical pulses using a spatial phase-only mask

The scheme is shown in Fig. 2: a spatial dispersion is applied by a grating on the input optical pulse, then a phase mask provides a spatial phase modulation and finally a spatial dispersion compensation is given by another grating. Its main drawback consisted in being a free space solution with all the problems related to a needful strict alignment, including significant insertion losses and limited integration with fiber or waveguide optics systems. For these reasons we looked for an all-fiber solution that essentially is a time-domain equivalent (Fig. 3) of the classical spatial-domain pulse shaping technique (Weiner et al., 1993), in which all-fiber temporal dispersion is used instead of spatial dispersion.

To achieve this all-fiber approach we started from a different solution based on the concept concerning a time-frequency mapping using linear dispersive elements (Azaña et al., 2005). As shown in Fig. 3 (top), applying an optical pulse at the input of a first order dispersive medium, we obtain an output signal $e_{disp}(t)$ dispersed in time domain corresponding to the spectral domain of the input pulse. In this way, a temporal phase modulation $\varphi(t)$ applied to the dispersed signal coming out from the dispersive medium corresponds to a spectral phase modulation $\Phi(\omega)$ applied to the input spectrum (Fig. 3, bottom). For a given first order chromatic dispersion coefficient β_2, the correspondence between temporal and spectral phase modulations is:

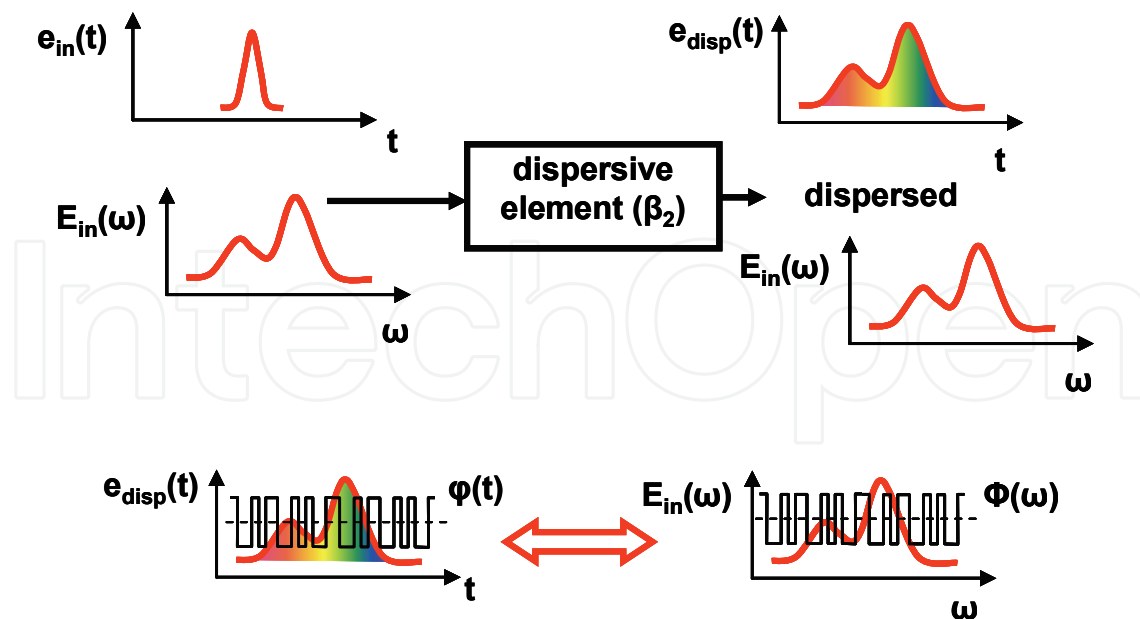$$\varphi(t) = \Phi(\omega = t/\beta_2) \tag{3}$$

Fig. 3. Principle of time-frequency mapping for the time-domain pulse shaping approach. β_2: first order dispersion coefficient; $\varphi(t)$: temporal phase modulation applied to the dispersed signal; $\Phi(\omega)$: spectral phase modulation applied to the input spectrum, corresponding to $\varphi(t)$

To apply the mentioned phase modulation an electro-optic (EO) phase modulator will be used. As it will be more clear afterwards, *any $\Phi(\omega)$ that satisfies Eq. 2 will not be practical* in terms of design and implementation. Therefore we restrict $\Phi(\omega)$ to a binary function with levels $\pi/2$ and $-\pi/2$ and a frequency resolution determined by practical system specifications (input/output dispersion and EO modulation bandwidth). It is possible to demonstrate that with such a binary phase modulation with levels $\pi/2$ and $-\pi/2$, the re-shaped signal is symmetric in the time domain. The temporal resolution of the binary phase code, similarly to Eq. 2, is related to the corresponding spectral resolution this way:

$$\omega_{pix} = T_{pix} / \beta_2 \tag{4}$$

Finally, to achieve the inverse Fourier-transform operation on the stretched, phase-modulated pulse, such a pulse is compressed back with a dispersion compensator providing the conjugated dispersion of the first dispersive element (Fig. 4).

As reported in Fig. 4, the binary phase modulation is provided to the EO-phase modulator by a bit pattern generator (BPG) with a maximum bit rate of 20 Gb/s.

Dispersion mismatch between the two dispersive conjugated elements has a negative effect on the performance of the system and for obtaining good quality pulse profiles it is critical to match these two dispersive elements very precisely. In our work, this was achieved by making use of the same linearly chirped fiber Bragg grating (LC-FBG) acting as pre- and post-dispersive element, operating from each of its two ends, respectively (Fig. 5); this simple strategy allowed us to compensate very precisely not only for the first-order dispersion introduced by the LC-FBG, but also for the present relatively small undesired higher-order dispersion terms.

As reported in Fig. 6, reflection of the LC-FBG acts as a band-pass filter applying at the same time a group delay (GD) versus wavelength that is linear on the reflected bandwidth. In

particular the slope of the two graphs of Fig. 6 (left) represents the applied first-order dispersion coefficient, respectively +480 and -480 ps/nm for each of the two ends of the LC-FBG.
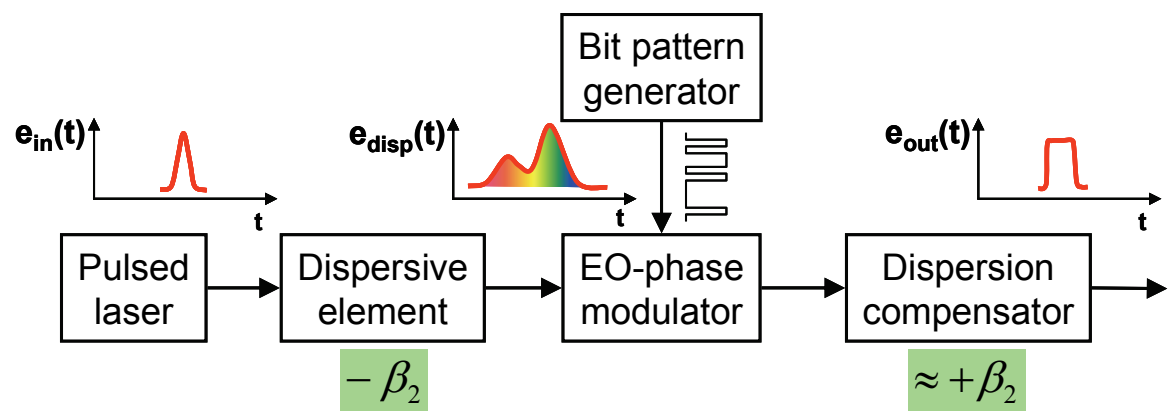

Fig. 4. Schematic of the pulse shaping concept based on time-frequency mapping and exploiting a binary phase-only filtering
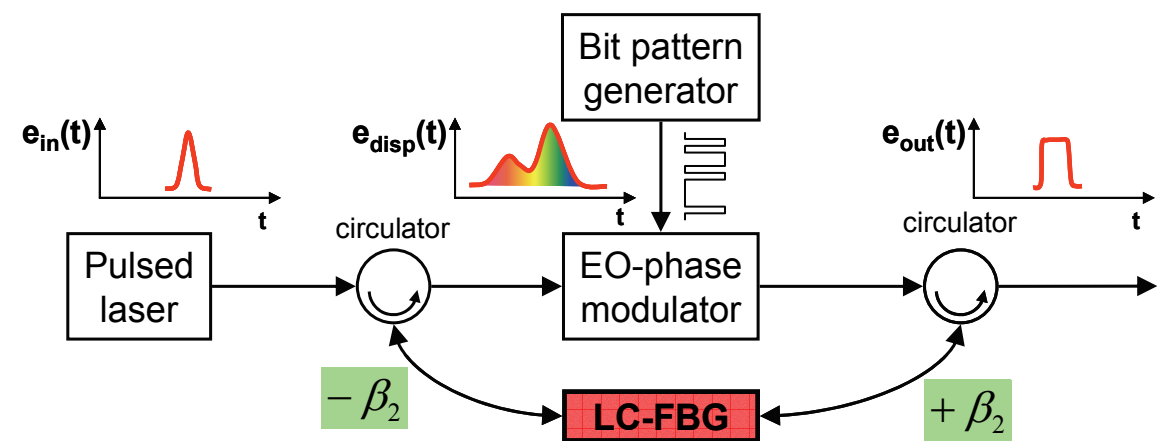

Fig. 5. Schematic of the pulse shaping concept based on time-frequency mapping exploiting a single LC-FBG as pre- and post-dispersive medium
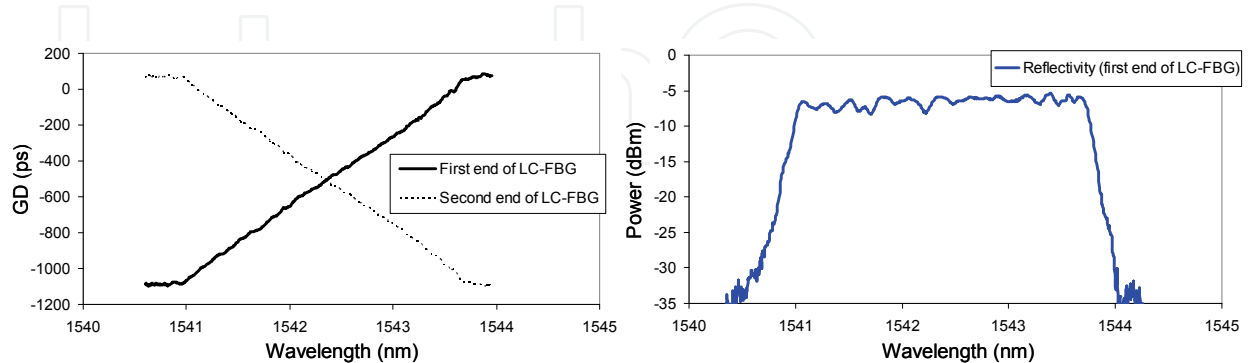

Fig. 6. Reflection behavior of the LC-FBG. (left) Group delay over the reflected bandwidth for both the ends; (right) reflected bandwidth of the first end

Similarly to any linear pulse shaping method, the shortest temporal feature that can be synthesized using this technique is essentially limited by the available input spectrum. On

the other hand, the maximum temporal extent of the synthesized output profiles is inversely proportional to the achievable spectral resolution $\omega_{pix.}$

2.1 Genetic algorithm as search technique

To find the required binary phase modulation function we implemented a genetic algorithm (GA) (Zeidler et al., 2001). A GA is a search technique used in computing to find exact or approximate solutions to optimization and search problems. GAs are a particular class of evolutionary algorithms that use techniques inspired by evolutionary biology such as inheritance, mutation, selection, and crossover (also called recombination), and they've been already exploited for optical pulse shaping applications (Wu & Raymer, 2006). They are implemented as a computer simulation in which a population of abstract representations (called *chromosomes*) of candidate solutions (called individuals) to an optimization problem evolves toward better solutions. Traditionally, solutions are represented in binary as strings of logic "0"s and "1"s. The evolution usually starts from a population of randomly generated individuals and happens in generations. In each generation, the fitness of every individual in the population is evaluated, multiple individuals are stochastically selected from the current population (based on their fitness), and modified (recombined and possibly randomly mutated) to form a new population. The new population is then used in the next iteration of the algorithm. Commonly, the algorithm terminates when either a maximum number of generations has been produced, or a satisfactory fitness level has been reached for the population. If the algorithm has terminated due to a maximum number of generations, a satisfactory solution may or may not have been reached.

In our case we use GA to find a convergent solution for phase codes corresponding to desired output intensity profiles (targets), starting from an input spectrum nearly Fourier transform-limited. First we code each spectral pixel with '0' or '1' according to the phase value ($\pi/2$ or $-\pi/2$, respectively). Each bit pattern producing a phase code is a chromosome. We start with 48 random chromosomes. We select the best 8 chromosomes in terms of their fitness (in terms of *cost function*, explained later). We obtain 16 new chromosomes from 8 pairs of old chromosomes (all of them chosen within the best 8) by *crossover* (2 new chromosomes from each pair). Then we obtain 24 new chromosomes from 24 random old chromosomes (1 new chromosomes from each) by *mutation*. Then we have 48 chromosomes again ("the best 8" + "16 from crossover" + "24 from mutation"). This iteration can be repeated a certain number of times. For our simulations we've chosen 10÷30 iterations corresponding to elaboration times in the range of 5÷15 seconds (10 iterations for flat-top and triangular pulses generation, 20÷30 iterations for bursts generation).

The fitness of each chromosome is indicated by its corresponding *cost function*. Each *cost function C_i* generally represents the maximum deviation in intensities between the predicted output signal $e_{out}(t)$ and the target $u(t)$ in a time interval $[t_i, t_{i+1}]$:

$$C_i = \max\left\{\left|e_{out}(t) - u(t)\right|\right\}; \quad t \geq 0 \; and \; t \in [t_i, t_{i+1}] \tag{5}$$

while the *total cost function C_{tot}* is defined as sum of the partial cost functions C_i, each of them with a specific weight w_i :

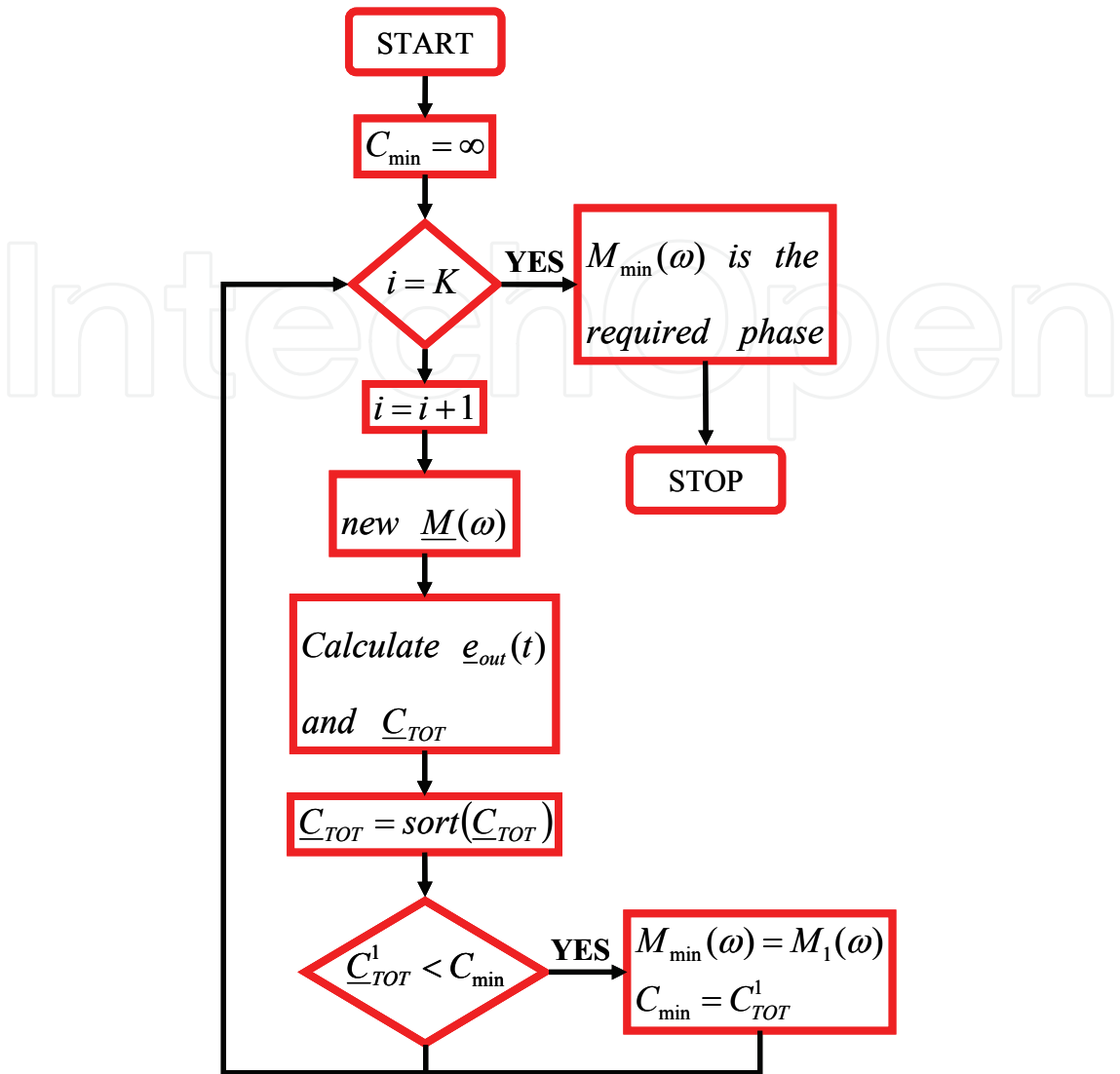$$C_{tot} = \sum_i C_i w_i \tag{6}$$

Fig. 7. Flow chart of the applied optimization technique

During each iteration, thanks to GA we move in a direction that reduces the total cost function. This way we derived the particular phase code so as to obtain the desired output temporal intensity profile, whose deviation from the target hopefully is within an acceptable limit. After a sufficient number of iterations, the obtained phase profile can be then transferred to the experiment. In Fig. 7 the flow chart for a general optimization technique is shown. In our case within the block where we calculate the new array of transfer functions $\underline{M}(\omega)$, we apply GA through crossover and mutation as explained above.

To better understand what a cost function is, we report here a couple of examples concerning the cost functions used for single flat-top pulse and pulsed-burst generations. In Fig. 8 (left) the features taken into account for a flat-top pulse generation are shown. Since the generated signal is symmetric in the time domain, we considered just the right half of the output profile.

Three time intervals correspond to three cost functions: the first one (C_1) is related to the flatness in the central part of the pulse, the second one (C_2) concerns the steepness of the falling edge, whereas the last one (C_4) is related to the pedestal amplitude. In particular, in Fig. 9(a) we report the comparison between the simulated temporal profile carried out

through GA and its relative theoretical target for the case of a flat-top pulse. In this case, the defined total cost function was $C_{tot}=5C_1+C_2+C_4$.
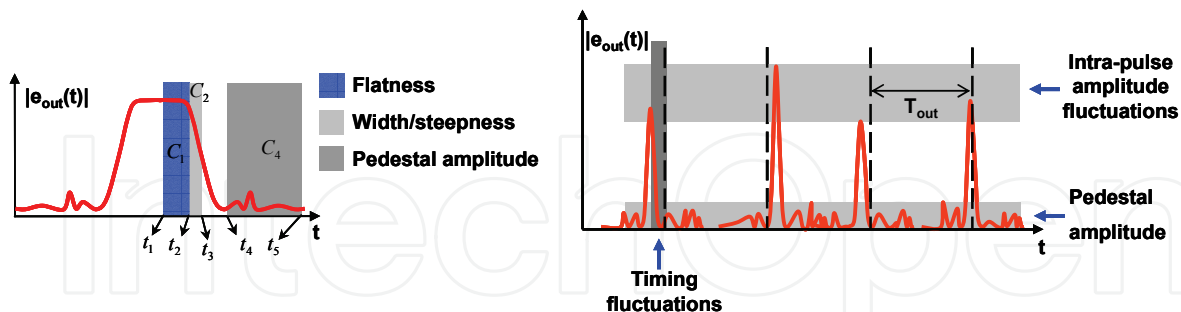

Fig. 8. (left) Cost functions for a single flat-top pulse generation. (right) Features taken into account with cost functions for a pulsed-burst generation
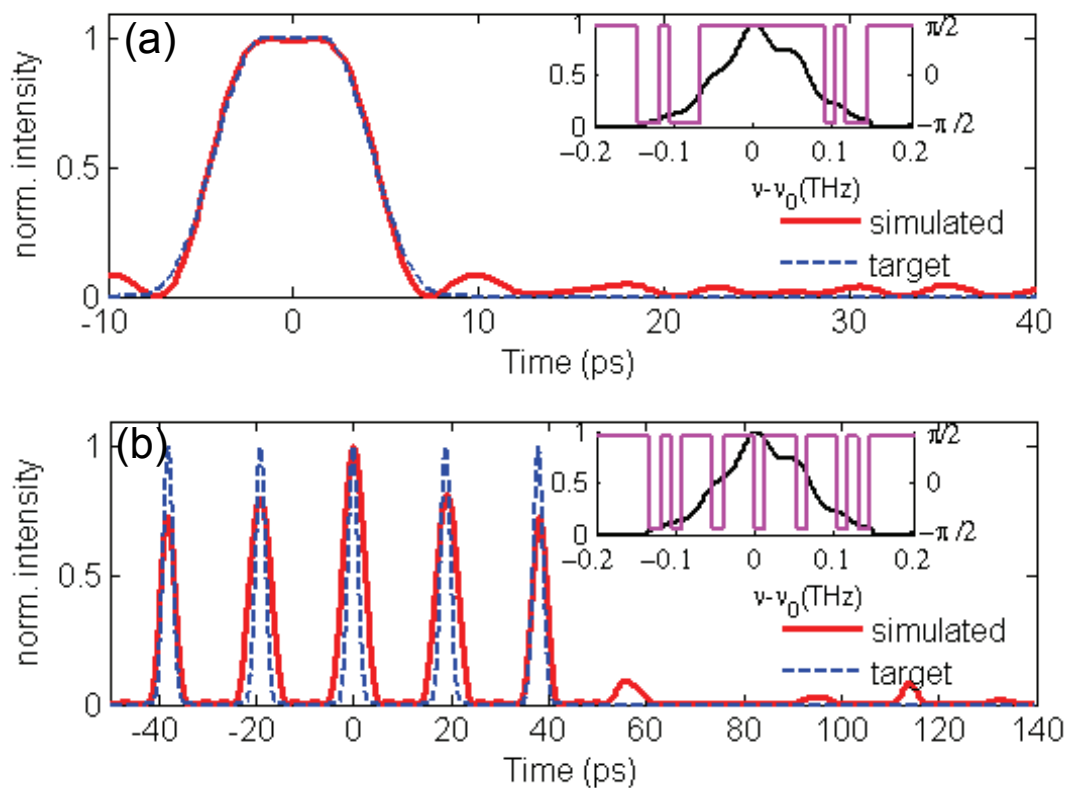

Fig. 9. Simulated and target profiles for a flat-top pulse (a) and a 5-pulses sequence (b). The used phase codes are shown in the insets (solid) together with the input pulse spectrum (dashed)

In Fig. 8 (right) another example considering a pulsed-burst as target shows the considered features: the intra-pulse amplitude fluctuations, the timing fluctuations and the pedestal amplitude again. In particular, Fig. 9(b) shows the comparison between the simulated temporal profile and its relative theoretical target for the case of a 5-pulses sequence. In this case, even though we weighted the partial cost functions in order to obtain a sequence with flat-top envelope, because of the limited spectral resolution, the simulated sequence is not so equalized (inter-pulse amplitude fluctuations $\approx 25\%$) as the theoretical target.

To demonstrate the programmability of the proposed scheme, we targeted shapes like flat-top, triangular and bursts of 2, 3, 4 and 5 pulses with nearly flat-top envelopes, defining a specific total cost function for each case.

2.2 Experimental setup

As shown in the experimental setup in Fig. 10, the exploited optical pulse source was an actively mode-locked fiber laser producing nearly transform-limited ~ 3.5 ps (FWHM) Gaussian-like pulses with a repetition rate of 10 GHz, spectrally centered at $\lambda_0 = 1542.4$ nm. The source repetition rate was decreased down to 625 MHz, corresponding to a period of 1.6 ns, using a Mach-Zehnder amplitude modulator (MZM) and a bit pattern generator (BPG 1) producing a binary string with a logic "1" followed by fifteen logic "0".
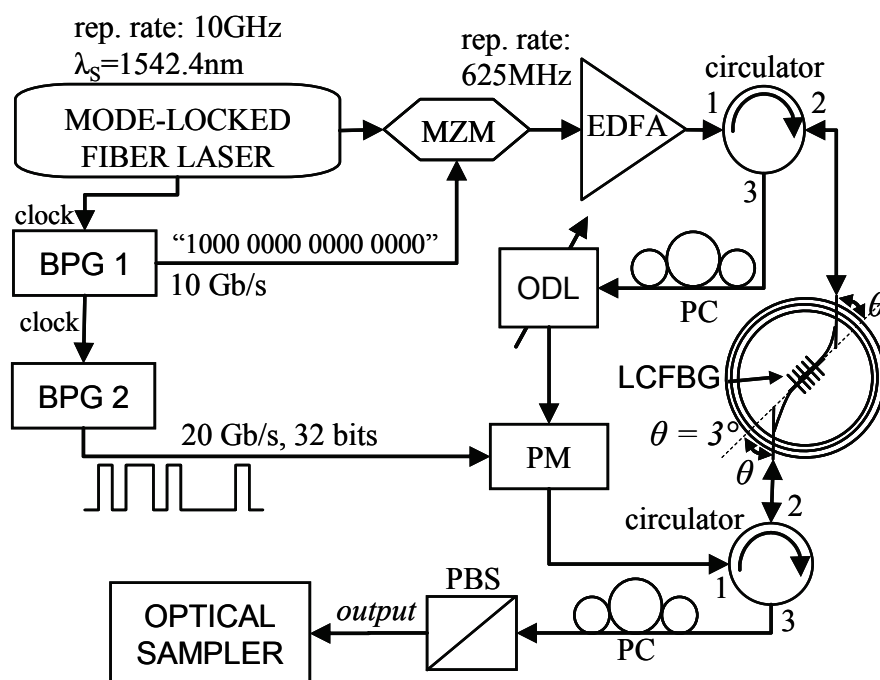

Fig. 10. Experimental setup of the programmable all-fiber pulse shaper

In order to temporally stretch the optical pulses, they were reflected in a LC-FBG, incorporated in a tunable mechanical rotator for fiber bending, which allowed us to tune the chromatic dispersion coefficient by changing the stretching angle θ (Kim et al. 2004). Such tunable dispersion compensator will be deepened and described in next Section (Section 2.2.1). Setting $\theta = 3°$, we obtained a first-order dispersion coefficient of 480 ps/nm ($\beta_2 \approx$ -606 ps^2/rad) over a 3dB reflection bandwidth of 2.3 nm (centered at the laser wavelength λ_0=1542.4nm). The dispersed pulses (port 3 of first circulator), each extending over a total duration of ~1.6 ns, were temporally modulated using an EO phase modulator (PM) driven by a second bit pattern generator (BPG 2), generating 32-bit codes, each with a bit rate of 20 Gb/s and a period of 1.6 ns, according to the designed codes obtained from the GA. To accurately synchronize the phase code and the stretched pulse we employed an optical delay line (ODL) together with shifting bit by bit the code generated from BPG 2. In order to precisely compensate for the previously applied chromatic dispersion value, we used the same LC-FBG operated in the opposite direction, thus introducing the exact opposite dispersion (-480 ps/nm). At port 3 of the second circulator we obtained the desired output

pulse together with a small amount of the input pulse transmitted through the grating. The desired output was discriminated using a polarization controller (PC) and a polarization beam splitter (PBS). Finally, the output temporal waveform was monitored by a commercial autocorrelator first, and then acquired by a quasi asynchronous optical sampler prototype (Section 6 of Fresi's chapter) based on four wave mixing (FWM), with a temporal resolution of ~ 100 fs.

2.2.1 Tunable dispersion compensator based on a LC-FBG

Referring to (Kim et al. 2004), a method to achieve tunable chromatic dispersion compensation without a center wavelength shift is based on the systematic bending technique along a linearly chirped fiber Bragg grating (LC-FBG). The bending curvature along the LC-FBG corresponding to the rotation angle of a pivots system can effectively control the chromatic dispersion value of the LC-FBG within its bandwidth. The group delay can be linearly controlled by the induction of the linear strain gradient with the proposed method. Based on the proposed method, the chromatic dispersion could be controlled in a range typically from ~100 to more than 1300 ps/nm with a shift of the grating center wavelength less than 0.03 nm over the dispersion tuning range.

In our particular case, to "write" the LC-FBG prototype exploited in the experiment presented in Section 2.2, we used a setup where a UV laser with a wavelength of 244 nm was employed. Its light beam was deflected by a sequence of mirrors; the last mirror was fixed on a mechanical arm, whose position was automatically driven by a proper LabView software, so as to hit a phase mask. Such a mask divided the input beam in two coherent beams so as to create interference fringes through beating. Such fringes had the task to photo-expose the span of fiber in order to realize the LC-FBG. In this case the linear chirp (periodicity linearly increasing/decreasing along the fiber) was directly introduced by the phase mask.

In Fig. 11 the measured reflection spectrum and the group delay (GD) of a typical LC-FBG are reported, showing excellent results in terms of amplitude ripples (< 0.5dB) (Fig. 11(a)) and linear behavior of the GD versus wavelength (Fig. 11(b)). The main difference between the LC-FBG described in this section and the one employed in Section 2.2 is the central wavelength (1542.4 nm instead of 1550.4 nm).
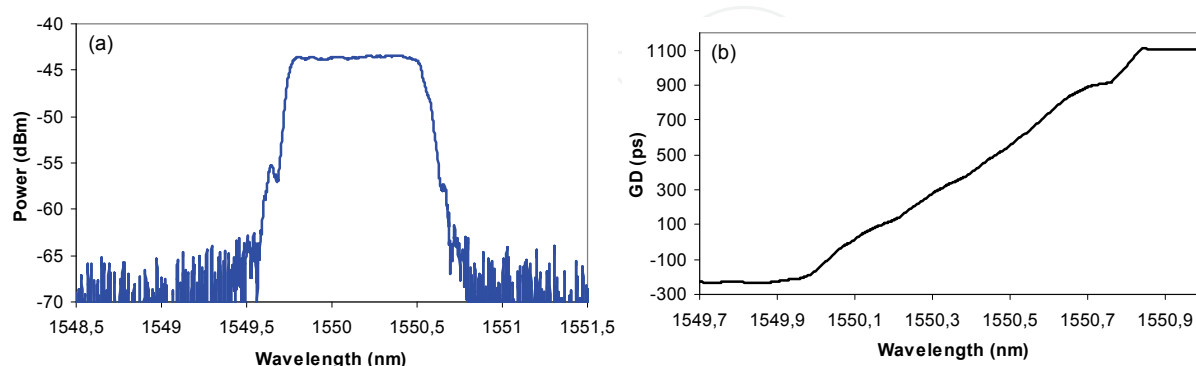

Fig. 11. (a) Reflection spectrum of a typical LC-FBG. (b) GD of the same LC-FBG

The LC-FBG was carefully attached to the cantilever beam fixed on the rotation stage in order to compose the dispersion-tuning device (Kim et al. 2004). Through the device a certain tunable bending angle is applied on the metal beam where the grating is attached.

Both the bandwidth and the chromatic dispersion value (the derivative of the graph in Fig. 11(b)) of the grating change with the bending angle applied to the grating. In particular, increasing the rotation angle it is possible to decrease the chromatic dispersion and to increase the reflection bandwidth.

In Fig. 12(a),(c) variation of reflection spectra with the rotation angle are shown, whereas in Fig. 12(b),(d) variation of GD with the rotation angle are reported. As shown in Fig. 12(a),(c), the central wavelength of the reflection bandwidth is fixed and equal to ~1550.4 nm. In Fig. 13 variation of the chromatic dispersion (left) and the -3dB-bandwidth (right) with the rotation angle are reported.
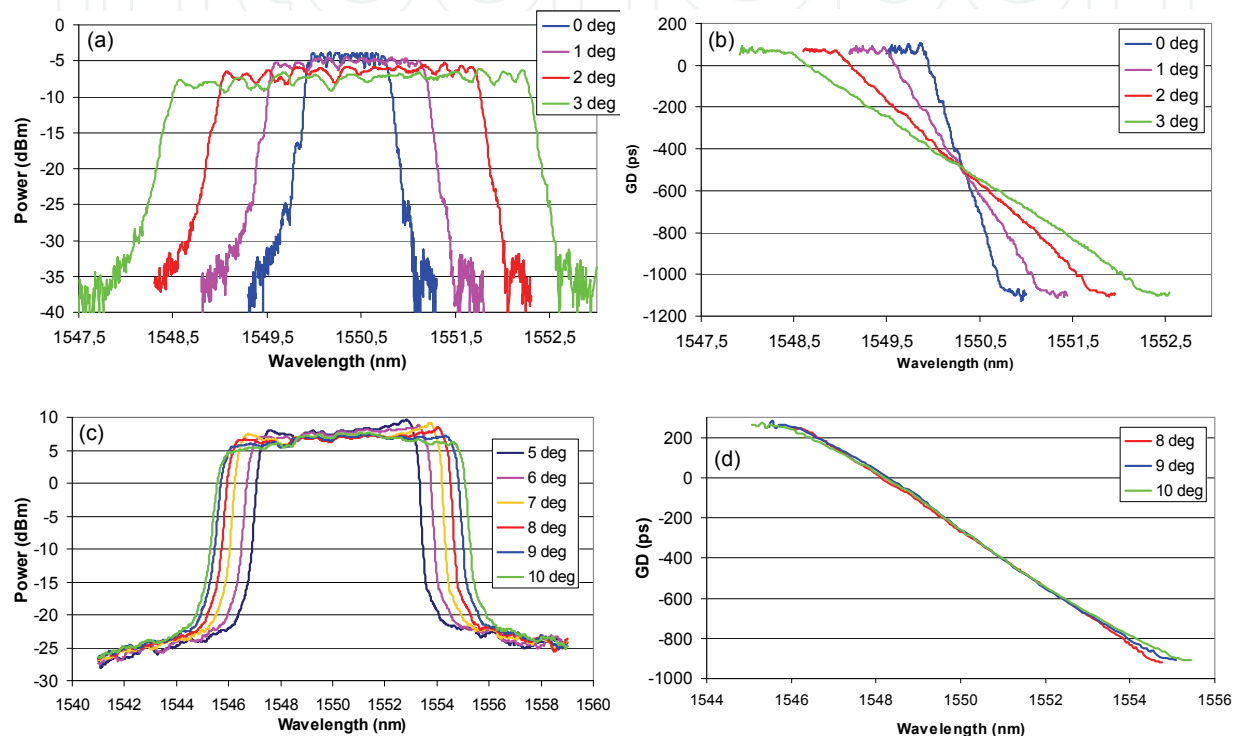

Fig. 12. Measured results of the variation of (a),(c) the reflection spectra and (b),(d) the group delay of the tunable dispersion compensator with the rotation angle
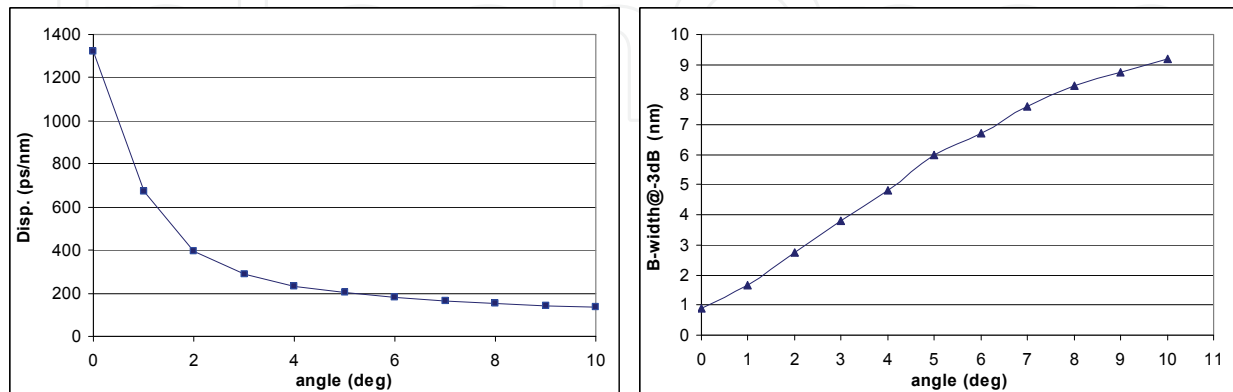

Fig. 13. Variation of chromatic dispersion (left) and -3dB-bandwidth (right) of the tunable dispersion compensator with the rotation angle

Concluding, in the example reported in this section a LC-FBG has been fabricated through a proper setup and it has been employed with a mechanical rotator in order to compose an all-fiber tunable chromatic dispersion compensator able to provide a chromatic dispersion in the range (±134.4;±1320.4) ps/nm. The sign of the applied chromatic dispersion depends on which end of the grating we employ. Furthermore, adding a circulator on an end of the LC-FBG, we obtain a system where port 1 and port 3 of the circulator represents the input and the output of the tunable dispersion compensator respectively (Fig. 14).
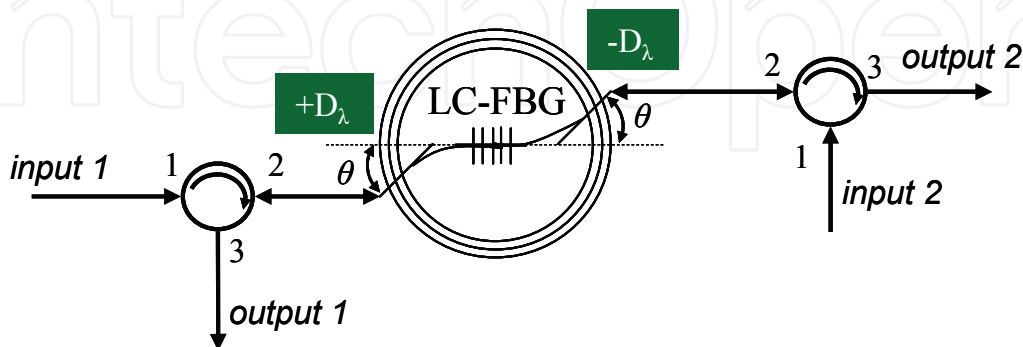

Fig. 14. Tunable chromatic dispersion compensator scheme. From input 1/output 1 a positive chromatic dispersion is provided whereas from input 2/output 2 a negative chromatic dispersion is provided

2.3 Experimental results

The capabilities of our programmable picosecond pulse re-shaping system were first demonstrated synthesizing the flat-top optical pulse related to Fig. 9(a) and the 5-pulses sequence related to Fig. 9(b), monitoring the temporal profile of the output signal through a commercial autocorrelator (Fig. 15), then the experiment has been repeated monitoring the output optical signal by an optical sampler. In particular we synthesized five different temporal waveforms of practical interest (Petropoulos et al., 2001; Park et al., 2006; Azaña et
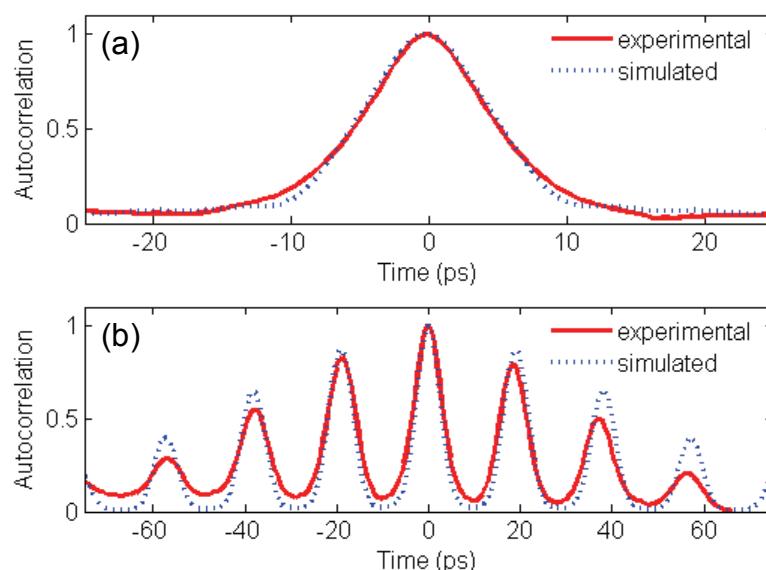

Fig. 15. Experimental and simulated autocorrelation curves for the flat-top pulse (a) and the 5-pulses sequence (b)

al., 2003) (see Fig. 16), namely a 9-ps (FWHM) flat-top optical pulse (Fig. 16(a)), a 8.5-ps (FWHM) triangular pulse (Fig. 16(b)), and three pulse sequences with flat-top envelopes, respectively a "11" (Fig. 16(c)), a "111" (Fig. 16(d)) and a "101" (Fig. 16(e)) sequence, with ~ 20-ps bit spacing.
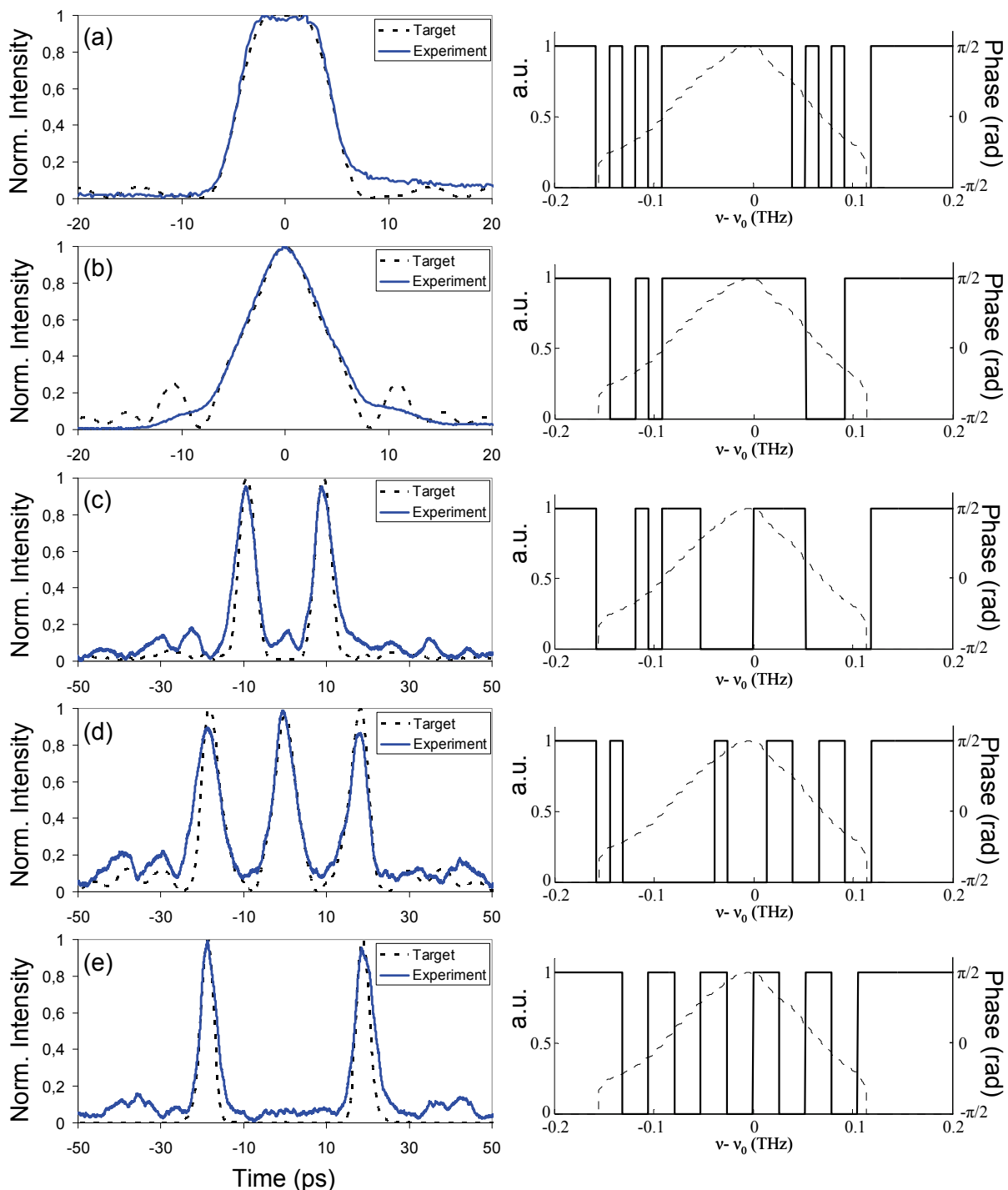

Fig. 16. Target and experimental profiles for a flat-top pulse (a), a triangular pulse (b), a "11" sequence (c), a "111" sequence (d) and a "101" sequence. The respective used phase codes are shown on the right (solid) together with the input pulse spectrum (dashed)

Fig. 16 shows the traces of the five synthesized pulse shapes experimentally acquired by the optical sampler in comparison with the simulated pulse shapes (the required binary codes to synthesize each of the target shapes are shown on the right of each graph), showing an excellent agreement between theory and experiments in all cases. Based on the values of the temporal pixel (the bit period of the BPG 2 was T_{pix} = 20 ps) and first-order dispersion used in our setup (D_λ = 480 ps/nm), we estimated a spectral resolution (Eq. 4) of ~ 13.1 GHz, which restricted the extension of the synthesized waveforms to ~ 76 ps, limiting the number of pulses per synthesized pulse burst, each with a repetition period of ~ 20 ps, to a maximum of three consecutive pulses.

To show the behavior of the system working on targets with a temporal extent larger than the above mentioned maximum, in Fig. 17 we report the comparison between simulated targets and experimental output temporal profiles acquired by the optical sampler, for cases with a temporal extent larger than 80 ps. In the first case (Fig. 17(a)) even though the agreement between simulation and experiment is quite good by the amplitude peaks of the target, the pulse shaper is not able to maintain the pedestal amplitude within an acceptable level, especially by the logic "0"s of the sequence. Moreover, in the target of the sequence "1001" two side residual peaks are already present due to a limited spectral resolution.
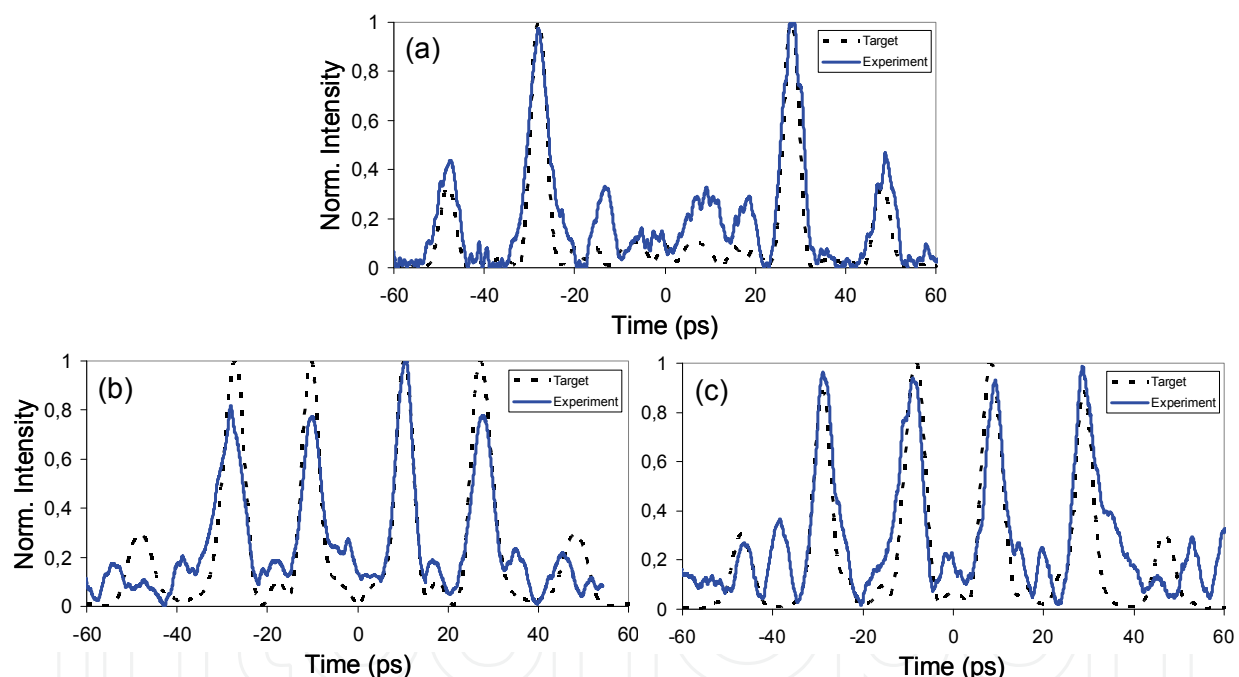

Fig. 17. Target and experimental profiles for a "1001" sequence (a), a "1111" sequence with an equalized target (b) and a "1111" sequence with a non-equalized target (c)

This limitation is due to the limited chromatic dispersion imposed by the LC-FBG (with a dispersion more than 480 ps/nm the reflection bandwidth would be narrower than the input signal bandwidth giving rise to unacceptable distortions on the output signal) and to the bit rate of the BPG 2 (20 Gb/s is the maximum value).

If we consider all the features mentioned in Section 2.1 about a pulsed-burst (acceptable pulses amplitude fluctuations, timing fluctuations, pedestal amplitude), having a look on Fig. 17(b)-(c) it is possible to notice bad performances in particular for the equalization and the pedestal level of the pulsed sequence. Moreover, the mismatch between simulated

targets and experimental results increased if compared with all the cases shown in Fig. 16, confirming the non-correct working condition.

Considering the frequency bandwidth of the output pulses from the pulse shaper (FWHM ≈ 4.5 ps corresponding to a bandwidth ≈ 222 GHz), the reported setup provided a fairly high time-bandwidth product > 16.

As indicated by Eq. 4, a higher spectral resolution (i.e. longer temporal extension for the synthesized waveforms) can be achieved by increasing the bit rate of BPG 2 or by use of a higher dispersion. Using a higher dispersion would however require to decrease the repetition rate of the generated output pulses (assuming the same input pulse bandwidth). Other experimental non-idealities affecting the system performance include spectral fluctuations of the input spectrum, the non-perfect squared shape of the electric binary code produced by the BPG 2 and undesired higher order dispersion terms introduced by the LC-FBG.

3. Conclusion

In conclusion, we have demonstrated a fiber-based time-domain linear binary phase-only filtering system enabling arbitrary temporal re-shaping of picosecond optical pulses. Flat-top and triangular pulses together with two and three pulse-bursts have been synthesized from the same input pulse by properly programming the bit pattern code driving an EO phase modulator.

4. References

Azaña, J.; Slavik, R.; Kockaert, P.; Chen, L.R.; LaRochelle, S. (2003). Generation of customized ultrahigh repetition rate pulse sequences using superimposed fiber Bragg grating. *IEEE Journal of Lightwave Technology*, Vol. 21, No. 6, (June 2003) 1490-1498, 0733-8724

Azaña, J.; Berger, N. K.; Levit, B.; Fischer, B. (2005). Reconfigurable generation of high-repetition-rate optical pulse sequences based on time-domain phase-only filtering. *Optics Letters*, Vol. 30, No. 23, (December 2005) 3228-3230, 0146-9592

Dai, Y.; Yao, J. (2008). Arbitrary pulse shaping based on intensity-only modulation in the frequency domain. *Optics Letters*, Vol. 33, No. 4, (February 2008) 390-392, 0146-9592

Kim, J.; Bae, J. K.; Han, Y. G.; Kim, S. H.; Jeong, J. M.; Lee, S. B. (2004). Effectively tunable dispersion compensation based on chirped fiber Bragg gratings without central wavelength shift. *IEEE Photonics Technology Letters*, Vol. 16, No. 3, (March 2004) 849-851, 1041-1135

Kurokawa, T.; Tsuda, H.; Okamoto, K.; Naganuma, K.; Takenouchi, H.; Inoue, Y.; Ishii, M. (1997). Time-space-conversion optical signal processing using arrayed-waveguide grating. *Electronics Letters*, Vol. 33, No. 22, (October 1997) 1890-1891, 0013-5194

Lin, I.S.; Weiner, A.M. (2007). Hardware Correlation of Ultra-Wideband RF Signals Generated via Optical Pulse Shaping, *IEEE International Topical Meeting on Microwave Photonics, 2007*, pp. 149-152, 1-4244-1168-8, Victoria, BC, Canada, October 2007

Otani, T.; Miyazaki, T.; Yamamoto, S. (2000). Optical 3R regenerator using wavelength converters based on electroabsorption modulator for all-optical network

applications. *IEEE Photonics Technology Letters*, Vol. 12, No. 4, (April 2000) 431-433, 1041-1135

Oxenlowe, L.K.; Slavik, R.; Galili, M.; Mulvad, H.C.H.; Park, Y.; Azana, J.; Jeppesen, P. (2007). Flat-top pulse enabling 640 Gb/s OTDM demultiplexing, *Proceedings of European Conference on Lasers and Electro-Optics, 2007 and the International Quantum Electronics Conference. CLEOE-IQEC 2007*, CI8-1, 978-1-4244-0931-0, Bourgogne, France, June 2007

Park, Y. and Azaña, J. (2006). Optical pulse shaping technique based on a simple interferometry setup, *Proceedings of 19th Annual Meeting of the IEEE Lasers & Electro-Optics Society, 2006*, pp. 274-275, 9780780395558, Montreal, QC, Canada, November 2006

Park, Y; Kulishov, M; Slavík, R; Azaña, J. (2006). Picosecond and sub-picosecond flat-top pulse generation using uniform long-period fiber gratings. *Optics Express*, Vol. 14, No. 26, (December 2006) 12670-12678, 1094-4087

Parmigiani, F.; Petropoulos, P.; Ibsen, M.; Richardson, D.J. (2006). All-optical pulse reshaping and retiming systems incorporating pulse shaping fiber Bragg grating. *IEEE Journal of Lightwave Technology*, Vol. 24, No. 1, (January 2006) 357-364, 0733-8724

Parmigiani, F.; Finot, C.; Mukasa, K.; Ibsen, M.; Roelens, M. A.; Petropoulos, P.; Richardson, D. J. (2006). Ultra-flat SPM-broadened spectra in a highly nonlinear fiber using parabolic pulses formed in a fiber Bragg grating. *Optics Express*, Vol. 14, No. 17, (August 2006) 7617-7622, 1094-4087

Petropoulos, P.; Ibsen, M.; Ellis, A.D.; Richardson, D.J. (2001). Rectangular pulse generation based on pulse reshaping using a superstructured fiber Bragg grating. *IEEE Journal of Lightwave Technology*, Vol. 19, No. 5, (May 2001) 746-752, 0733-8724

Wang, X. and Wada, N. (2007). Spectral phase encoding of ultra-short optical pulse in time domain for OCDMA application. *Optics Express*, Vol. 15, No. 12, (June 2007) 7319-7326, 1094-4087

Weiner, A. M.; Oudin, S.; Leaird, D. E.; and Reitze, D. H. (1993). Shaping of femtosecond pulses using phase-only filters designed by simulated annealing. *Journal of the Optical Society of America A*, Vol. 10, No. 5, (May 1993) 1112-1120, 0740-3232

Weiner, A. M. (1995). Femtosecond optical pulse shaping and processing. *Progress in Quantum Electronics*, Vol. 19, No. 3, (1995) 161-237, 0079-6727

Wu, C.; Raymer, M.G. (2006). Efficient picosecond pulse shaping by programmable Bragg gratings. *IEEE Journal of Quantum Electronics*, Vol. 42, No. 9, (September 2006) 873-884, 0018-9197

Zeidler, D.; Frey, S.; Kompa, K.-L.; and Motzkus, M. (2001). Evolutionary algorithms and their application to optimal control studies. *Physical Review A*, Vol. 64, No. 2, (August 2001), 1050-2947
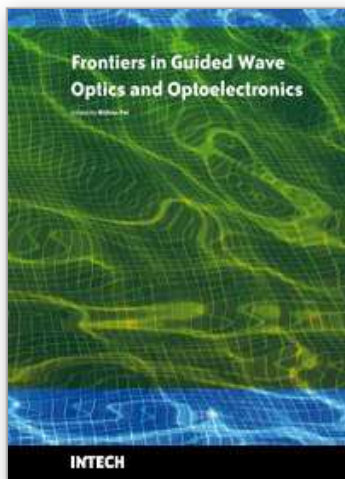
Frontiers in Guided Wave Optics and Optoelectronics

Edited by Bishnu Pal

ISBN 978-953-7619-82-4

Hard cover, 674 pages

Publisher InTech

Published online 01, February, 2010

Published in print edition February, 2010

As the editor, I feel extremely happy to present to the readers such a rich collection of chapters authored/co-authored by a large number of experts from around the world covering the broad field of guided wave optics and optoelectronics. Most of the chapters are state-of-the-art on respective topics or areas that are emerging. Several authors narrated technological challenges in a lucid manner, which was possible because of individual expertise of the authors in their own subject specialties. I have no doubt that this book will be useful to graduate students, teachers, researchers, and practicing engineers and technologists and that they would love to have it on their book shelves for ready reference at any time.

How to reference

In order to correctly reference this scholarly work, feel free to copy and paste the following:

Antonio Malacarne, Saju Thomas, Francesco Fresi, Luca Potì, Antonella Bogoni and Josè Azaña (2010). Programmable All-Fiber Optical Pulse Shaping, Frontiers in Guided Wave Optics and Optoelectronics, Bishnu Pal (Ed.), ISBN: 978-953-7619-82-4, InTech, Available from: http://www.intechopen.com/books/frontiers-in-guided-wave-optics-and-optoelectronics/programmable-all-fiber-optical-pulse-shaping

INTECH
open science | open minds